Space Shuttle Stability and Control Derivatives Estimated from the First Entry

Kenneth W. Iliff* and Richard E. Maine†
NASA Ames Research Center, Edwards, California
and
Douglas R. Cooke‡
NASA Johnson Space Center, Houston, Texas

The primary stability and control derivative estimates obtained from the first Space Shuttle entry are presented in this report. Data range from before entry interface to Mach 1.5. The derivative estimates were obtained using a maximum likelihood estimation program. The results from the first flight are not completely definitive because there were no intentional maneuvers designed for stability and control derivative estimation. The data obtained were adequate to establish the viability of the data system and estimation technique and to show most of the major trends. The flight results largely agreed with predictions, with a few exceptions. The stability and control maneuvers planned for subsequent flights should provide the accuracy and confidence required for the routine operational use of the Shuttle.

Nomenclature

a_n, a_x, a_y	= normal, longitudinal, and lateral accelerations, respectively, g
C_l	= rolling moment coefficient
C_m	= pitching moment coefficient
C_n	= yawing moment coefficient
DJ	= downfiring jets, number of jets
h	= altitude, ft
L	= rolling moment, ft-lbf
M	= Mach number
$M_{( )}$	= pitching moment as a function of ( ), ft-lbf
N	= yawing moment, ft-lbf
p	= roll rate, deg/s
q	= pitch rate, deg/s
$\bar{q}$	= dynamic pressure, lbf/ft^2
r	= yaw rate, deg/s
t	= time, s
UJ	= upfiring jets, number of jets
YJ	= yaw jets, number of jets (left minus right is positive)
α	= angle of attack, deg
β	= angle of sideslip, deg
δ_a	= differential elevon deflection, deg, (left − right)/2
δ_{BF}	= body flap deflection, deg
δ_e	= average elevon deflection, deg
θ	= pitch angle, deg
Φ	= roll angle, deg

Subscripts

$DJ, UJ, YJ, \alpha, \beta, \delta a, \delta e$	= partial derivatives with respect to the subscripted variable

Paper 81-2451 presented at the AIAA/SETP/SFTE/SAE First Flight Testing Conference, Las Vegas, Nev., Nov. 11-13, 1981. Submitted Nov. 20, 1981; revision received Oct. 22, 1982. This paper is the work of the U.S. government and therefore is in the public domain.

*Senior Staff Scientist, Dryden Flight Research Facility. Associate Fellow AIAA.

†Aerospace Engineer, Dryden Flight Research Facility. Member AIAA.

‡Aerospace Engineer, Engineering and Development Directorate.

Introduction

THE first flight of the Space Shuttle included unique and important information concerning aircraft flight dynamics. Maneuvering manned flight over a wide range of hypersonic velocities was demonstrated for the first time. These data have provided the opportunity to assess flight characteristics in completely new flight regimes. Among the flight characteristics to be assessed are the stability and control derivatives. The only maneuvers obtained during the first entry were those required to enter and land safely. No special maneuvers were performed specifically for the purpose of providing data for estimating stability and control derivatives.

Estimation of the stability and control derivatives can be used in flight envelope expansion, to update simulators, to enhance maneuvering capability and flying qualities, and to provide the information necessary to improve the flight control system. In the case of the Shuttle, these derivatives are required to determine if certain configuration placards (limitations on the flight envelope) can be modified. Many of these placards involve the longitudinal and lateral center-of-gravity limits. The placards have been determined on the basis of preflight predictions and their associated uncertainties. As flight-determined derivatives are obtained, the placards can be reassessed, and, in many cases, it is hoped that many of them can then be removed or modified.

This paper presents flight-determined stability and control derivatives from the first Space Shuttle entry and compares them with the preflight predicted derivatives. Data for a Mach number range of 25 to 1.5 and an altitude range of 515,000 to 50,000 ft are presented in this paper. The Shuttle stability and control derivatives for low-altitude subsonic conditions were determined during the Shuttle approach and landing tests (ALT).[1,2] Very little maneuvering was done below a Mach number of 1.5 on the first Shuttle flight so no new estimates were obtained.

Vehicle Description

The Space Shuttle (Fig. 1) is 122 ft long with a wingspan of 78 ft. The entry control sytem consists of 12 vertical reaction control system (RCS) jets (six downfiring and six upfiring), eight horizontal RCS jets (four to the left and four to the right), four elevon surfaces, a body flap, and a split rudder surface. The locations of these devices are shown in Fig. 1. The RCS jets are rocket engines used to control the attitude of

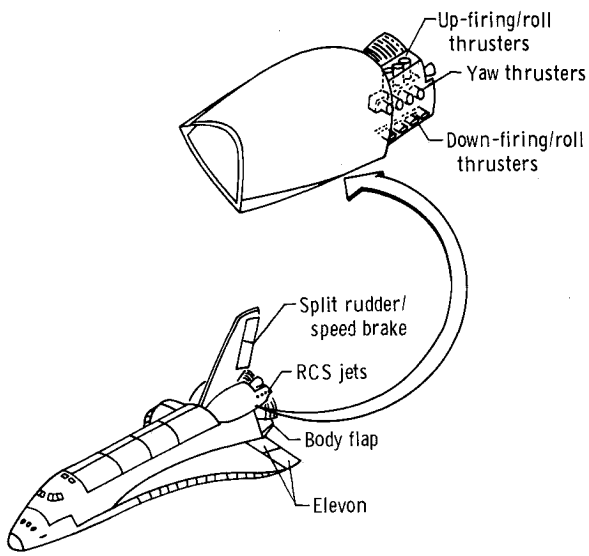

Fig. 1 Shuttle configuration.

the Shuttle. The vertical jets and the elevons are used for both pitch and roll control. The jets and elevons are used symmetrically for pitch control and asymmetrically for roll control. The body flap, used as a secondary pitch trim control, helps maintain the predetermined elevon schedule as a function of flight conditions. The rudder and side firing (yaw) jets provide directional control. The split rudder also functions as the speed brake. The vertical jets operate in roll (roll jets) only for dynamic pressures of less than 10 psf. The yaw jets are active when the Mach number is greater than 1.0. The body flap and elevons become active at a dynamic pressure of 0.51 psf. The rudders were used only at Mach numbers below 3.5.

Predictions

The predicted stability and control derivatives are presented in Ref. 3. In addition to the predicted values of the derivatives, Ref. 3 also contains estimates of the uncertainty in the predictions. These uncertainties are called "variations." The variations are based on the evaluation of previous correlations between wind-tunnel and flight-determined derivatives for aircraft of approximate delta-winged planform. The variations in Ref. 3 are based in part on the study of wind-tunnel and flight correlations presented in Ref. 4. The RCS jet moments are the sum of the pure thrust plus the interaction and impingement effects.

Table 1 Instrumentation properties

Measurement	Sample rate, samples/s	Source	Resolution	Bits
p	174	ACIP	0.004	14
q,r	174	ACIP	0.001	14
a_x	174	ACIP	0.0002	14
a_y	174	ACIP	0.00006	14
a_n	174	ACIP	0.0004	14
$\dot{p}$	174	ACIP	0.01	14
$\dot{q},\dot{r}$	174	ACIP	0.007	14
Elevons	174	ACIP	0.004	14
Rudder	174	ACIP	0.003	14
Body flap	1	GPC	0.04	10
RCS jets	25	OI	0.004	8
α	1	GPC	–	–
β	5	GPC	–	–
Euler angles	5	GPC	–	–
Flight condition	1	GPC	–	–

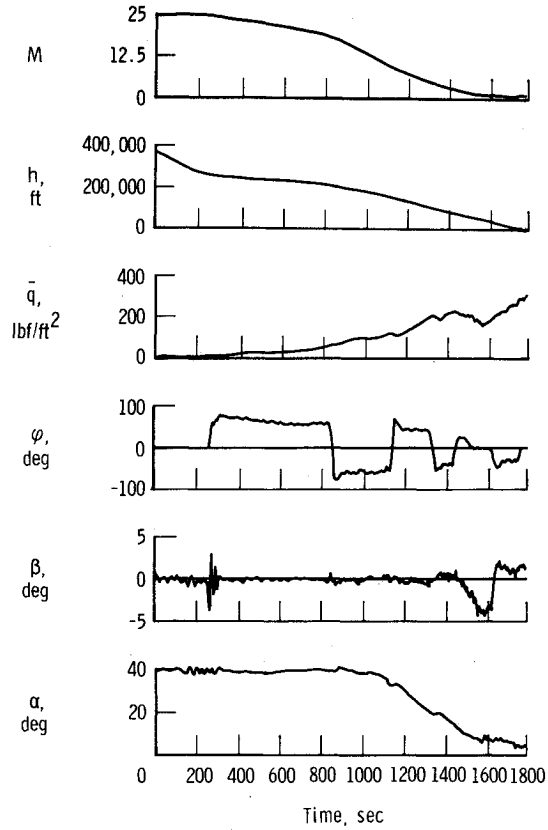

Fig. 2 Entry time-history ($t = 0$ at 17:50:00).

Flight Data System

The Shuttle flight data used for stability and control derivative estimation were recorded on three separate onboard systems. The primary data were recorded on the aerodynamic coefficient identification package (ACIP).[5] This package was specifically intended for providing high-quality data at a high sample rate to enhance the stability and control derivative estimates. A second system recorded data from the onboard general purpose computer (GPC) to provide the parameters defining the flight condition and the vehicle Euler angles. For Mach numbers greater than approximately 3, the "Mach number" from the GPC is actually computed as velocity divided by 1000. (All "Mach numbers" quoted in this paper use the GPC values for consistency.) The third system was the operational instrumentation (OI) system. Measurements of the RCS jet chamber pressures were obtained from this system. The chamber pressures are used because they reflect the thrust buildup and decay. The RCS jet time-histories presented in this paper are sums of the chamber pressures divided by the nominal single chamber pressure; for nominal conditions this gives the number of jets firing. Table 1 shows the data source of the important signals used in the analysis and the individual sample rates and measurement resolutions. The resolution of the ACIP parameters allows the analysis of some very small maneuvers. The results of the analysis of some of the small maneuvers will be discussed in a later section.

The data from the three sources were corrected for time skew, converted to engineering units, and then merged into a single file with a constant sample rate.

Figure 2 shows time-histories of the primary parameters defining flight condition for the entry from 370,000 ft to landing. All time-histories in this paper show time relative to the start of the plot; the start time (Greenwich Mean Time) is indicated on the plots. All of these signals were computed by the inertial measurement unit (IMU) and recorded on the GPC system. The large changes in bank angle (bank reversals)

are used for trajectory energy management. It should be noted that there were no external sources of the standard air data parameters on the Shuttle for the early part of the entry, so the inertially measured quantities were used for defining the flight condition. Any errors in the inertial parameters, in dynamic pressure particularly, will have corresponding effects on the stability and control derivative estimates. It should also be pointed out that below a Mach number of 3 the inertially determined sideslip angle was affected by wind, resulting in significant errors of up to 4.5 deg. The ground-based meteorological data showed wind shears below 75,000 ft, with winds as high as 50 ft/s. External side probes are extended at a Mach number of approximately 3.5 to provide improved air data, but this information was not used to correct sideslip angle. Therefore, the lateral-directional characteristics below Mach 3 are subject to some interpretation. As stated before, the output of the GPC was used for all of the analysis in this paper.

Method of Analysis

Today the primary method of obtaining estimated derivatives from flight data is the maximum likelihood estimation[6] or the output error method. The results for the first Shuttle flight were obtained from the maximum likelihood estimation program, MMLE3.[7] The Shuttle is modeled by a set of dynamic equations containing unknown stability and control derivatives. The equations used are those of Ref. 7, except that dimensional derivatives are used for RCS jets. To determine the values of the unknown derivatives, the vehicle needs to be excited by a suitable control input, and the input and the spacecraft response are both measured.

The values of the derivatives are then inferred based on the requirement that the mathematical model response to the input match the actual Shuttle-measured response. The Cramer-Rao bound[8] gives an indication of the accuracy of these values. The mathematical formulation of the technique used in the following analysis is contained in Refs. 6 and 7. Some of the practical implications of applying the MMLE3 program to flight data are contained in Refs. 9 and 10.

Flight Maneuvers

The primary goal of the highly successful first Space Shuttle flight was to demonstrate its ability to enter and return from orbit and to land horizontally. Therefore, the first flight was appropriately planned very conservatively, and intentional stability and control maneuvers were not included. Because of the uncertainties and complexities of attaining the primary goal, additional maneuvers would have imposed added risk to the success of the flight. Later flights, including the second, will show an emphasis on performing stability and control maneuvers. These maneuvers will be directed at improving the understanding of the aircraft in regions where flight placards on the flight envelope currently restrict the overall utility of the vehicle. In spite of the lack of intentional stability and control maneuvers, the motions obtained from the first flight were adequate to provide a significant new understanding of the stability and control characteristics of the vehicle.

The maneuvers with the greatest amount of motion were the planned bank reversals. These maneuvers were designed to produce very little in the way of dynamic vehicle response. The bulk of the lateral-directional stability and control derivatives were estimated from the bank reversals and many of the longitudinal derivatives also were extracted from the reversals. There was very little longitudinal motion for the entire entry; therefore, maneuvers of very small amplitude had to be relied upon for any flight-determined longitudinal stability and control derivatives. Fortunately this problem had been foreseen and the ACIP instrumentation package was designed to provide adequate resolutions and sample rates for obtaining information from these small maneuvers.

Longitudinal Maneuvers

The most apparent longitudinal motion was the oscillation during the first 300 s shown in Fig. 2, between Mach numbers of 25 and 24 and between altitudes of 350,000 and 250,000 ft. Although the oscillation was fairly small, it was the largest dynamic longitudinal motion during the entire entry. This oscillation is plotted in more detail in Fig. 3. The dynamic pressure started at about 0.5 psf when the elevons and body flap were activated and ended at 17 psf. The oscillation appears to result from an out-of-trim condition at entry interface and the resulting dynamic interaction between the body flap, the pitch jets, and the elevons. The body flap moved from its initial value of 7 deg to the final trim value of 16 deg. Because of the length of the oscillation and the large variation of dynamic pressure, the oscillation was divided into several shorter maneuvers for derivative estimation.

An example of a match for an extremely small maneuver is shown in Fig. 4. This maneuver was performed at a Mach number of 21.7. Longitudinal forces and moments due to angle of attack, elevon, and yaw jets were estimated. The noise on the measured responses is quite significant in comparison to the response. In spite of this, the match is still excellent and reasonable derivative estimates were obtained. Many of the derivatives in the next section were estimated from similar small maneuvers showing the value of the high-resolution ACIP instrumentation system for the application of the MMLE 3 program to Shuttle-type responses.

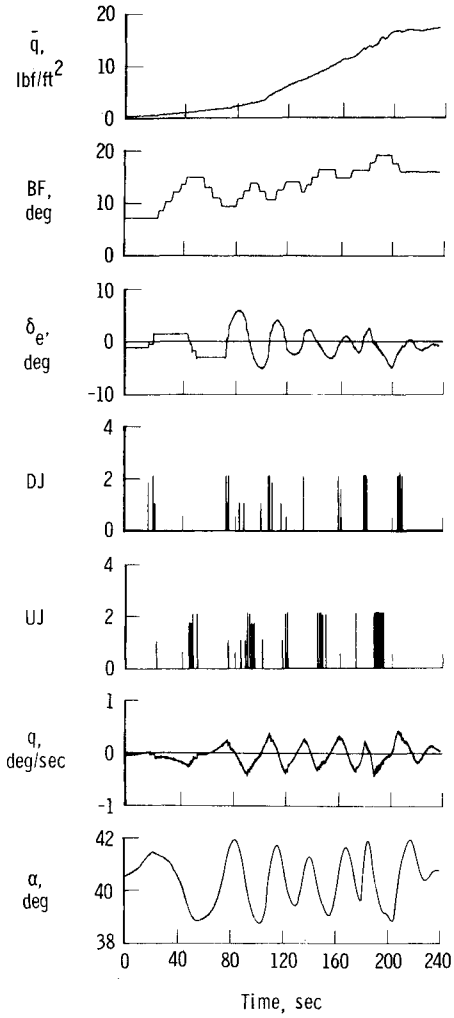

Fig. 3 Small longitudinal oscillation during interface ($t=0$ at 17:51:30).

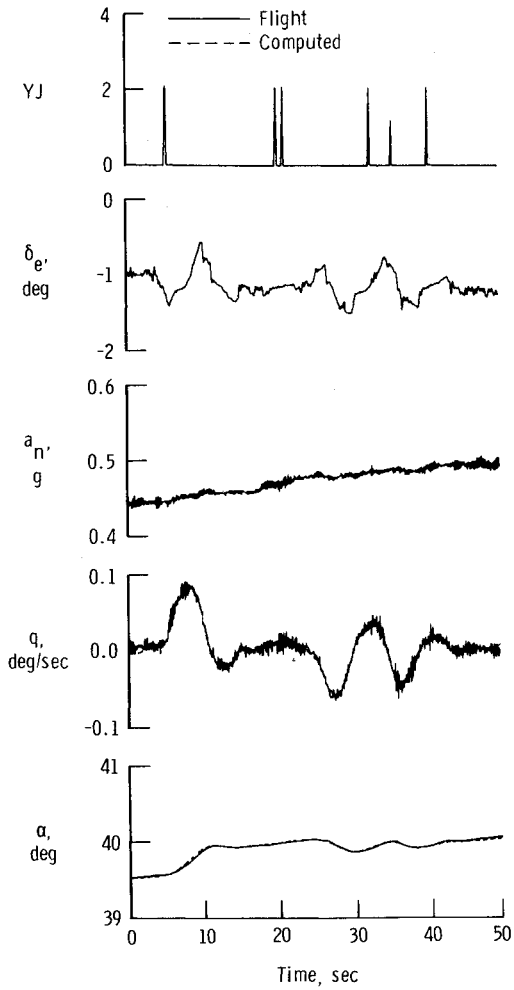

Fig. 4 Longitudinal match of small-amplitude maneuver ($t=0$ at 17:59:56).

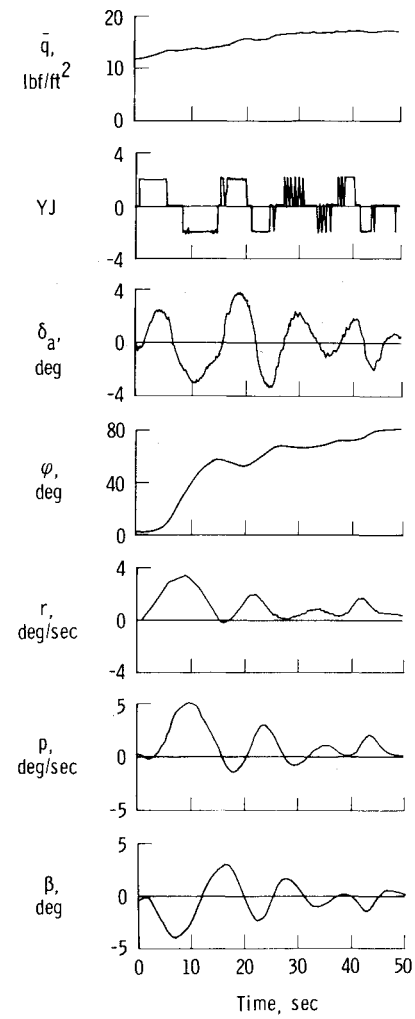

Fig. 5 Lateral-directional oscillation at $M=24$ bank reversal ($t=0$ at 17:54:25).

Lateral-Directional Maneuvers

The most apparent sideslip activity in Fig. 2, with the exception of the excursions in inertial sideslip below a Mach number of 3, occurs in the region from approximately 250 to 300 s. This time also corresponds to the end of the longitudinal oscillation previously discussed and the beginning of the first bank reversal. This maneuver, with sideslip excursions as high as 4 deg, could be characterized as a lightly damped, closed-loop, lateral-directional oscillation. Although the maneuver is considered quite large for this flight condition, the control system damped it out after several cycles. It was not felt that this excursion posed any major safety problem to the vehicle. The maneuver was of major interest for derivative extraction, with good longitudinal and lateral-directional derivatives extracted from this activity.

This oscillation is shown in more detail in Fig. 5, which illustrates the dynamic pressure to be increasing from 12 to 17 psf. The yaw jets and the differential elevons are very active during the maneuver. The initial peak of more than 3 deg/s in yaw rate and 5 deg/s in roll rate is as high as was observed during the entire entry. Stability and control derivative analysis (MMLE3) was applied to the entire oscillation with mostly satisfactory results, though the resulting time-history match was not as good as desired. This problem could be attributed to many effects such as nonlinearities or, in this particular case, to errors in the inertially derived dynamic pressure. Fairly small errors in dynamic pressure measurement can affect the estimates and the match for the entire oscillation. To minimize these effects, the oscillation was broken into two maneuvers. The first maneuver contained the largest variation in dynamic pressure and the largest amplitude in the response variables. The second maneuver was selected so that the dynamic pressure varied by less than 0.5 psf, the absolute value of the sideslip stayed below 1.5 deg, and the absolute value of differential elevon stayed below 2 deg.

Both of these maneuvers were analyzed with MMLE3 and had excellent matches. The two resulting sets of derivatives are shown in the next section. Figure 6 illustrates the match for the second part of the maneuver. It is felt that this maneuver is most representative of the Shuttle in its normal flight envelope, so the derivatives from this maneuver have been selected as being the most representative for a Mach number of 24. The derivatives extracted from this maneuver were the lateral-directional forces and moments due to sideslip, differential elevon, and yaw jets. Excellent matches were obtained for the high-quality roll and yaw accelerations.

Derivative Results

In this section the stability and control derivative estimates obtained from the flight are compared with predictions. Due to length limitations, not all of the derivatives estimated are presented.

The complicated functional dependence of the derivatives predicted in Ref. 3 cannot be validated by the data from a single flight. The predictions are a function of many parameters defining the flight condition, parameters such as Mach number, angle of attack, altitude, dynamic pressure,

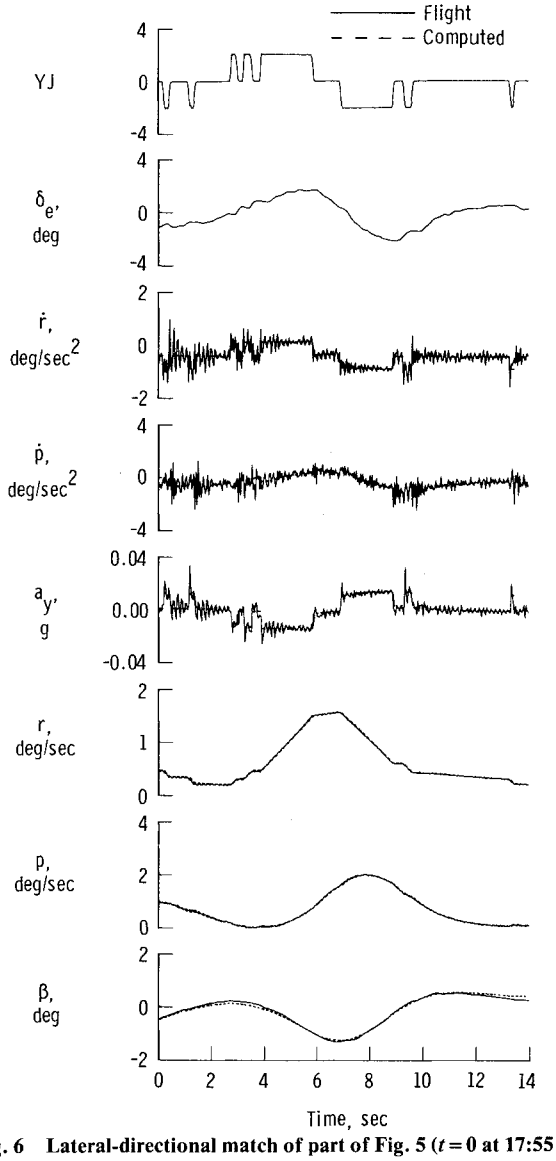

Fig. 6 Lateral-directional match of part of Fig. 5 ($t = 0$ at 17:55:01).

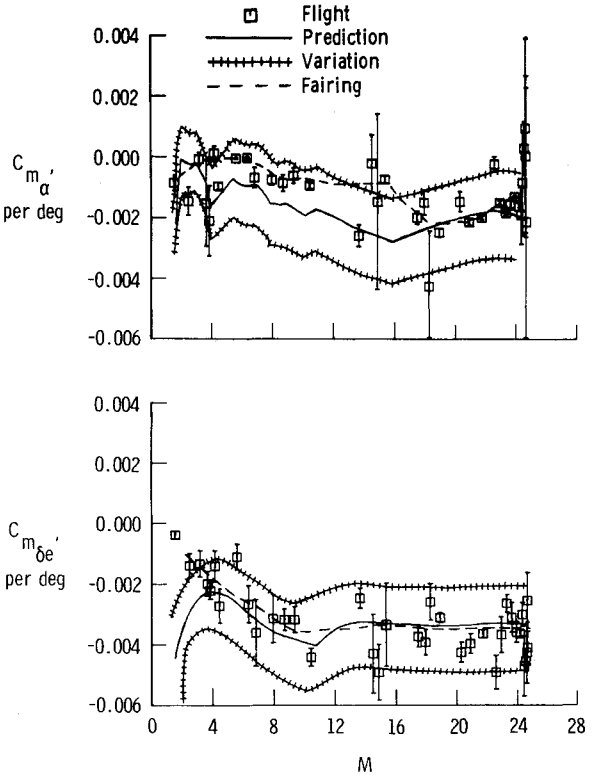

Fig. 7 Estimates of C_{m_α} and $C_{m_{\delta e}}$.

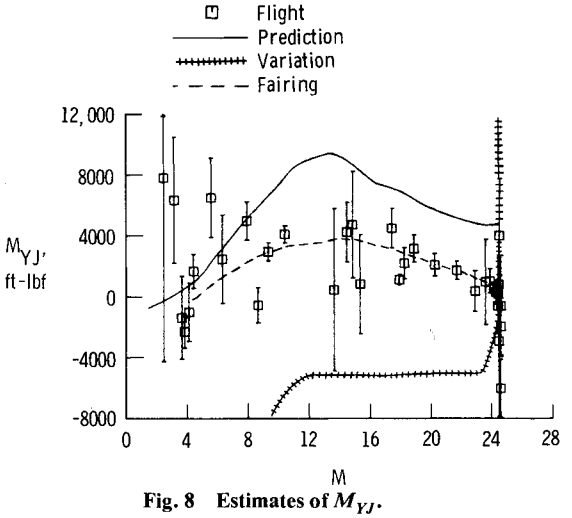

Fig. 8 Estimates of M_{YJ}.

body flap position, and elevon deflection. Between entry interface and final approach, the Mach number monotonically decreased from above 24 to below 1. Thus, for any particular Mach number, flight data are available only at a single value of angle of attack, dynamic pressure, altitude, body flap position, and other parameters.

Figure 2 can be used to find some of the important flight condition parameters corresponding to a given Mach number. Since several of these parameters are continually changing, it is not possible to conclusively attribute any trends observed in the derivatives to effects of specific flight condition parameters. Most of the estimates presented in this report are plotted as a function of Mach number; some data near entry interface, where Mach number is almost constant, are plotted as a function of dynamic pressure. This form of presentation is adopted only for convenience—it is not meant to imply that the trends observed are necessarily directly related to Mach number. For instance, the trends between Mach numbers of 12 and 2 may be more influenced by the angle of attack, which decreases from 40 to 10, than by the Mach number. The predictions shown on the plots are evaluated at the particular flight conditions occurring at each Mach number (or dynamic pressure) on the flight. Thus, the predictions shown are comparable to the flight results. All data presented are referenced to the actual flight center of gravity of 16.95% of chord.

The effects of rotary derivatives are very small for the high-speed flight regimes. Primarily for this reason, all the maneuvers were analyzed with the rotary derivatives at the predicted nominal values of Ref. 3. Therefore, at Mach numbers below 3.5, where the rotary derivatives begin to have some effect, any errors in the predicted rotary derivatives affect the estimates of other derivatives. This effect would appear primarily in the control derivative estimates, since changes in these derivatives would best account for errors in the rotary derivatives. It is not expected that this effect would be noticeable above a Mach number of 3. The rotary derivatives were not determined below a Mach number of 3 because, with no intentional stability and control maneuvers, the control and rotary derivatives were found to be nearly dependent.[9] The RCS yaw jet derivatives were determined throughout the entry, offering a significant set of flight data on RCS jet interference effects. RCS pitch and roll jets were active only during the early portions of the entry. It should

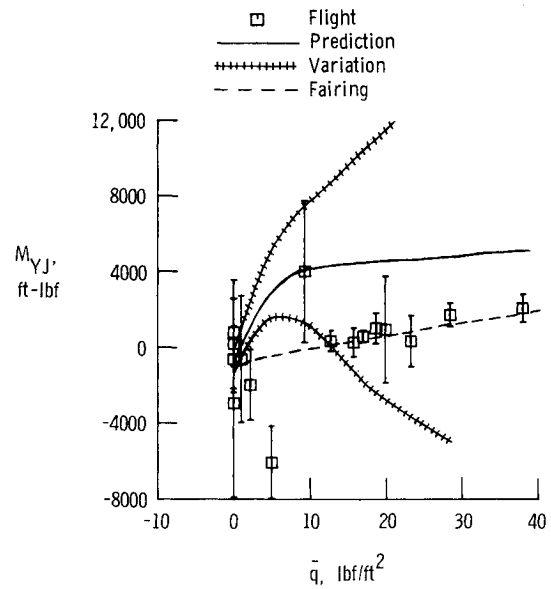

Fig. 9 Estimates of M_{YJ} at low dynamic pressure.

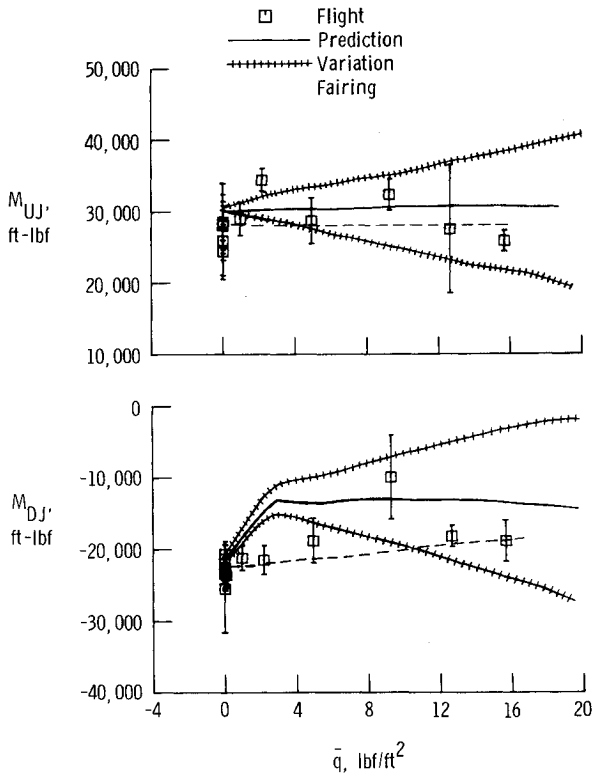

Fig. 10 Estimates of M_{UJ} and M_{DJ}.

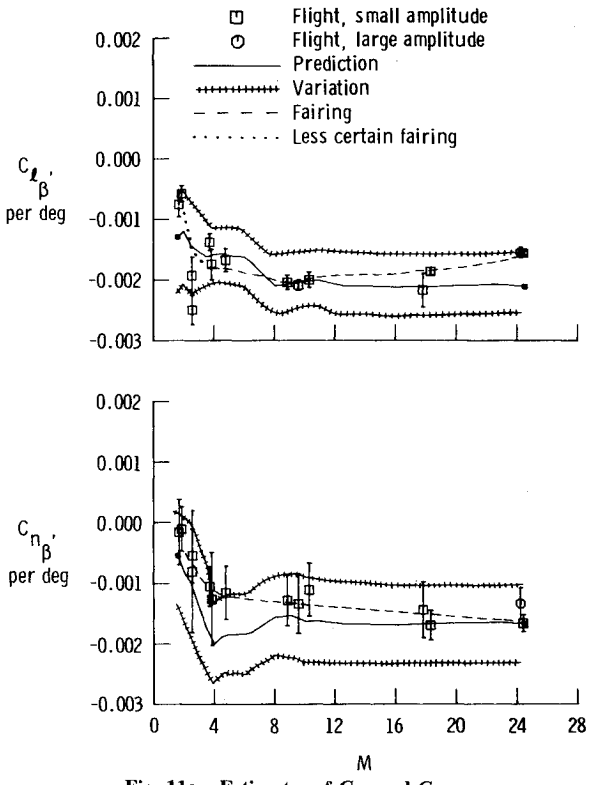

Fig. 11a Estimates of C_{l_β} and C_{n_β}.

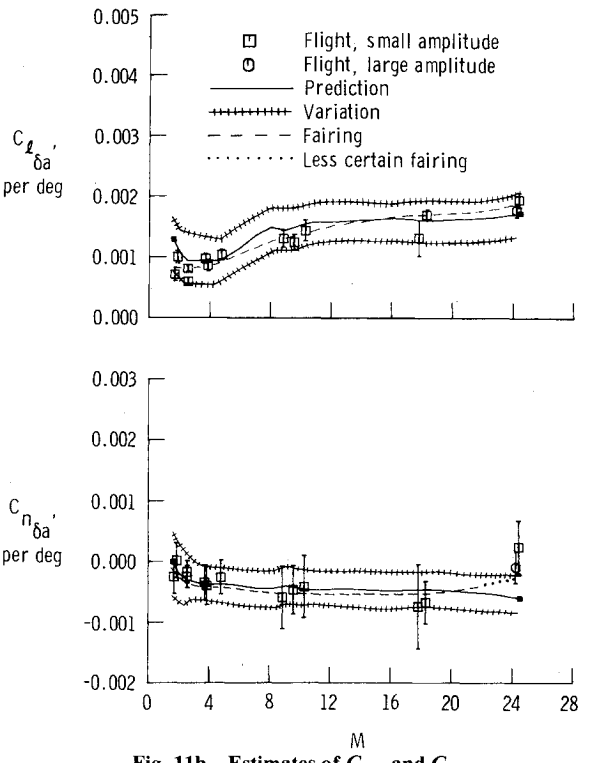

Fig. 11b Estimates of $C_{l_{\delta a}}$ and $C_{n_{\delta a}}$.

once again be pointed out that dynamic pressure, altitude, velocity, and angles of attack and sideslip are all GPC parameters from the inertial measurement unit; any errors in these parameters will result in errors in the estimated stability and control derivatives. Below Mach 2, buffet which degrades the accuracy of the derivative estimates was encountered.

In all of the following figures, a standard format is followed. The derivatives are, for the most part, plotted as a function of Mach number, although a few of the derivatives are plotted against dynamic pressure. The value of an estimate itself is represented by a symbol, and the uncertainty level[9,10] is represented by a vertical bar (the larger the uncertainty level, the less reliable the estimate). The uncertainty level is three times the calculated Cramer-Rao bound. A value of 3 was chosen since there were not a great deal of data and the maneuvers were not ideal for derivative estimation. If the uncertainty boundary exceeds the value of the vertical scale of a plot, it is terminated with an arrow instead of a flat bar. The solid fairing represents the nominal predictions, and the hatched solid lines represent the variations.[3] The dashed line is the fairing of the flight-determined derivatives; it changes to a dotted line where there is the greatest uncertainty. The forces due to the RCS jets are in pounds per jet, and the

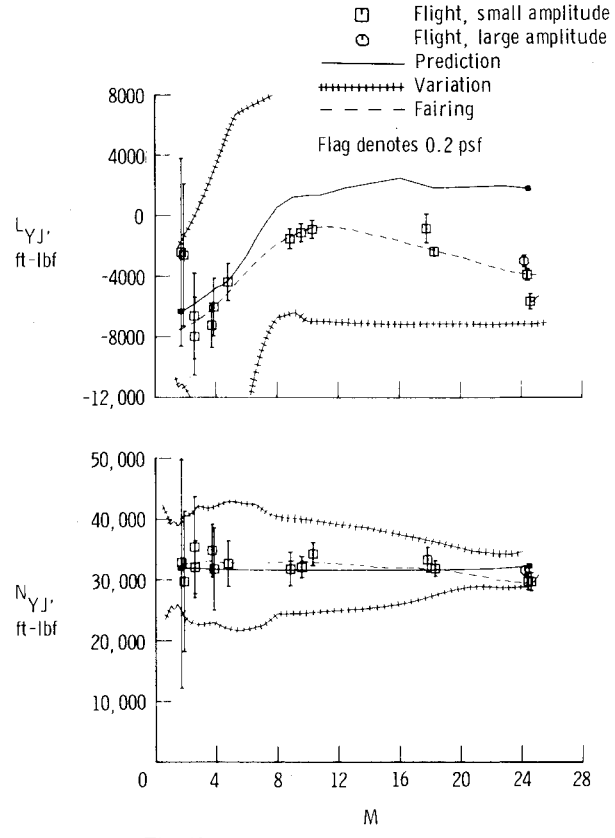

Fig. 12 Estimates of L_{YJ} and N_{YJ}.

moments are in foot-pounds per jet. All other derivatives are given per degree.

Longitudinal Derivatives

The most significant longitudinal stability and control derivative estimates are presented in Figs. 7-10. Figure 7 shows C_{m_α} and $C_{m_{\delta e}}$ as a function of Mach number. This presentation format is used for convenience, as pointed out earlier.

Above a Mach number of 24, the data scatter becomes quite large due to the low dynamic pressure. This unavoidable uncertainty is manifested in all of the longitudinal aerodynamic derivatives above a Mach number of 24 and will not be commented on for the subsequent plots. C_{m_α} agrees well with predictions above a Mach number of 17 and below 3. Between Mach numbers of 3 and 17, the flight C_{m_α} estimates show less stability than predicted, although they lie mostly within the variations. Between the Mach numbers of 11 and 17, the fairing is subject to some question and will require more maneuvers to give confidence in it. $C_{m\delta e}$ agrees well with predictions, but the scatter in the flight estimates is quite large. More accurate flight estimates are anticipated from the intentional stability and control maneuvers planned for subsequent flights. One point at a Mach number of 1.5 is well outside of the variation and has a small bound. Further maneuvers will be required to verify or contradict this point.

The cross-control derivative M_{YJ} is presented in Fig. 8. M_{YJ} is negative at the start of the entry and increases to about 4000 ft-lbf between Mach numbers of 10 and 15. As Mach number decreases further, M_{YJ} appears to decrease toward zero. The flight estimates of M_{YJ} are significantly different than predicted. They lie within the variations, but only because the variations are extremely large (off-scale for the positive variation). The fairing of M_{YJ} above a Mach number of 20 can better be appreciated by examining the same data plotted in Fig. 7 as a function of dynamic pressure for all points of dynamic pressure less than 40 psf. (Dynamic pressure less than 40 psf corresponds to Mach numbers greater than about 20, as shown in Fig. 2.) For the data during this part of the entry, dynamic pressure is probably a more meaningful parameter than Mach number. The flight fairing at low dynamic pressure agrees quite well with the vacuum thrust value of -856 ft-lbf. The flight data show a trend in the same direction as the predictions but quite different in shape. The flight data appear approximately linear with dynamic pressure below a dynamic pressure of approximately 40 psf.

The pitching moments of the up- and downfiring RCS jets are shown in Fig. 10 as a function of dynamic pressure. These jets were used only at dynamic pressures below 20 psf. The downfiring jets show a possible weak dependence on dynamic pressure in the same direction as predicted. As with the yaw jets, the dynamic pressure effect on M_{DJ} appears more nearly linear than predicted. The evidence is not as definitive for the downfiring jets as it was for the yaw jets because of the smaller number of points. No dynamic pressure dependence can be ascertained from the data available for the upfiring jets. The downfiring jet moments are significantly less than the vacuum thrust value of $-31{,}140$ ft-lbf, indicating that the jet impingement effects are significant. The predicted downfiring jet moment at zero dynamic pressure includes jet impingement effects and agrees well with the flight estimates.

Lateral-Directional Derivatives

Two problems, in addition to the aerodynamic buffet previously mentioned, affected the lateral-directional analysis below a Mach number of 3.5. The first problem was due to the activation of the rudder and the associated feedback systems at a Mach number of 3.5. The pilot made no independent rudder inputs, creating a situation of "near linear dependence."[9] Because of this situation, the MMLE3 program is unable to distinguish accurately between the effects of control motions (control derivatives) and the effects of feedback response variables (stability derivatives).

The second problem occurred because the only sideslip measurement is from the inertial system, which does not account for winds. The derivative estimation is adversely affected where winds are present. Winds were noticeable on the sideslip measurement below a Mach number of 3.

In summary, the data suitable for lateral-directional derivative estimation below a Mach number of 3.5 are limited for the following reasons: 1) no independent rudder motions; 2) wind contamination of the sideslip measurement; and 3) aerodynamic buffet (primarily below a Mach number of 2).

In Figs. 11 and 12, the squares all indicate low-amplitude excursions, while the one circle shown on most of the plots is for the large-amplitude portion of the lateral oscillation maneuver discussed in the Flight Maneuvers section. The fairings go through the small-amplitude estimates, since it is felt that this is the best estimate of the normal Shuttle flight envelope.

Figure 11 shows C_{l_β}, C_{n_β}, $C_{l_{\delta a}}$, and $C_{n\delta a}$ as functions of Mach number. The previous discussion concerning why the trends are not necessarily induced by Mach number still applies. C_{l_β} agrees fairly well with the predictions, showing values somewhat closer to zero below a Mach number of 4 and above a Mach number of 16. The flight fairing and most of the estimates are within the variations. The flight values of C_{n_β} indicate a more rapid trend toward increasing stability as Mach number decreases than do the predictions and are close to the upper variation near a Mach number of 4. $C_{l\delta a}$ is in good agreement throughout the Mach number range, although it is somewhat larger than predicted at high Mach numbers and somewhat lower in Mach numbers below 4. In all cases it is within the variations. $C_{n\delta a}$ shows good agreement between flight and prediction except for the highest Mach number where it is outside the variation.

Figure 12 shows L_{YJ} and N_{YJ} as functions of Mach number. The flagged symbol indicates the value for very low dynamic pressure ($\bar{q}=0.2$ psf). L_{YJ} from flight is in fair agreement with predictions for Mach numbers less than 8 and

then becomes negative with Mach number while the prediction becomes positive. This should result in a noticeably different response than that predicted. All values are within the variations. The estimate for the 0.2 psf point is in very good agreement with the vacuum thrust value of −6370 ft-lbf. N_{YJ} from flight is in good agreement with predictions everywhere and falls inside the variations in all cases except at a Mach number of 24.

The flight-determined lateral-directional derivatives are in good agreement with predictions in almost all cases except at Mach numbers below 3.5 and at the highest Mach number. The exception to this is L_{YJ}, which indicates a trend significantly different than that predicted. The lack of good agreement for most of the derivatives at Mach numbers of 3.6 and below could be due to poor damping predictions, wind shear or apparent wind shear, and/or buffet. The poor correlation at a Mach number of 24 could be due to nonlinearities, dynamic pressure effects, or errors in the measurement of inertial quantities. The answers to these questions and many others should be forthcoming from future flights on which specific stability and control maneuvers will be flown.

Concluding Remarks

This paper has presented the estimates of the stability and control derivatives obtained from the first Space Shuttle entry. This analysis demonstrated the ability to estimate derivatives in hypersonic flight for a large manned winged entry vehicle. Extremely small dynamic motions were successfully analyzed because of the high resolution instrumentation package. The general trends in the Shuttle derivative predictions have been validated, with the greatest disagreement with predictions found in the reaction control system jet aerodynamic interaction effects. Good lateral-directional results were difficult to obtain below a Mach number of 3 because of wind shear, buffet, and linear dependence problems. In order to further validate the predictions, specific stability and control maneuvers will need to be performed in critical areas of the flight envelope on subsequent flights.

References

[1] Hoey, R.G. et al., "AFFTC Evaluation of the Space Shuttle Orbiter and Carrier Aircraft NASA Approach and Landing Test," AFFTC-TR-78-17, May 1978.

[2] Cooke, D.R., "Subsonic Stability and Control Flight Test Results of the Space Shuttle (Tail Cone Off)," AIAA Paper 80-1604, Aug. 1980.

[3] "Aerodynamic Design Data Book, Orbiter Vehicle STS-1," SD72-5H-0060 Revision M, Space Division, Rockwell International, Nov. 1980.

[4] Weil, J. and Powers, B.G., "Correlation of Predicted and Flight Derived Stability and Control Derivatives—With Particular Application to Tailless Delta Wing Configurations," NASA TM-81361, July 1981.

[5] "ACIP End Item Specification," BD 2359202, Bendix Aerospace Systems Operations, Ann Arbor, Mich., 1980.

[6] Iliff, K.W. and Taylor, L.W. Jr., "Determination of Stability Derivatives from Flight Data Using a Newton-Raphson Minimization Technique," NASA TN D-6579, 1972.

[7] Maine, R.E. and Iliff, K.W., "User's Manual for MMLE3, A General FORTRAN Program for Maximum Likelihood Parameter Estimation," NASA TP-1563, 1980.

[8] Maine, R.E. and Iliff, K.W., "The Theory and Practice of Estimating the Accuracy of Flight-Determined Coefficients," NASA RP-1077, 1981.

[9] Iliff, K.W., Maine, R.E., and Montgomery, T.D., "Important Factors in the Maximum Likelihood Analysis of Flight Test Maneuvers," NASA TP-1459, 1979.

[10] Iliff, K.W., "Aircraft Identification Experience," AGARD LS-104, 1980.